ELSEVIER

Journal of Molecular Catalysis A: Chemical 140 (1999) 199–214

JOURNAL OF MOLECULAR CATALYSIS A: CHEMICAL

Studies of the adsorption of acetaldehyde, methyl acetate, ethyl acetate, and methyl trifluoroacetate on silica

M.A. Natal-Santiago, Josephine M. Hill, J.A. Dumesic *

Department of Chemical Engineering, University of Wisconsin, Madison, WI 53706, USA

Received 24 March 1998; accepted 29 June 1998

Abstract

Microcalorimetric, infrared spectroscopic, and temperature-programmed-desorption studies are combined with quantum-chemical calculations based on density-functional theory (DFT) to study the adsorption of acetaldehyde, methyl acetate, ethyl acetate, and methyl trifluoroacetate on amorphous silica. Adsorption of these molecules on silica proceeds primarily through formation of two hydrogen bonds per adsorbate, involving the donation of electron density from the lone-pair orbital on the carbonyl oxygen to hydrogen atoms in surface hydroxyl groups. The formation of these hydrogen bonds causes shifts to lower wavenumbers of infrared bands associated with the stretching of C=O and O–H bonds. On the basis of microcalorimetric and thermal-desorption measurements, hydrogen bonds are estimated to have an average energy of 34 ± 4 kJ/mol for methyl or ethyl acetate adsorption, and an energy of 27 ± 4 kJ/mol per bond for the adsorption of acetaldehyde or methyl trifluoroacetate. The initial heats of adsorption of methyl acetate, ethyl acetate, and methyl trifluoroacetate are 95, 96, and 92 (± 5) kJ/mol, respectively. These high heats of adsorption at low coverages are assigned, based on DFT calculations and spectroscopic measurements, to the formation of more than two hydrogen bonds with the oxide surface, thereby involving the alkoxy oxygen of the esters. The high initial heat of acetaldehyde adsorption (86 kJ/mol) may be caused by oligomerization processes.

Keywords: Adsorption of esters and acetaldehyde; Silica; Microcalorimetry; Fourier-transform infrared spectroscopy (FTIR); Temperature-programmed desorption (TPD); Density-functional theory (DFT)

1. Introduction

The adsorption and desorption of esters and aldehydes on metal oxides is important in relation to their synthesis over metal-oxide-based catalysts. For example, the partial reduction of acetic acid to acetaldehyde, as well as the selective oxidation of acetaldehyde to acetic acid, take place on silica, alumina, and other metal oxide catalysts [1,2]. In addition, esters are commonly prepared by esterification reactions involving a carboxylic acid and an alcohol [3]. While the most common catalysts used for esterification reactions are strong mineral acids such as sulfuric and hydrochloric acids, environmental factors favor the replacement of these corrosive liquids with solid acid catalysts [4], such as cation-exchange resins and zeolites [3].

The adsorption of carbonyl-containing organic compounds such as aldehydes [1,5–11], esters [12–15], ketones [5,7,16–21], and car-

* Corresponding author. Tel.: +1-608-2621095; Fax: +1-608-2625435; E-mail: dumesic@engr.wisc.edu

1381-1169/99/$ - see front matter
PII: S1381-1169(98)00231-3

boxylic acids [17] on amorphous silica has been studied extensively in the literature. Most of these investigations have utilized infrared spectroscopic measurements to characterize various surface species. In addition, Ugliengo et al. [10] have performed quantum-chemical calculations to elucidate the interactions between formaldehyde and isolated silanol groups. It is generally agreed that carbonyl-containing compounds adsorb on silica by forming hydrogen bonds involving the oxygen atom of the carbonyl group and hydroxyl groups on the oxide surface. Moreover, Rochester and coworkers [16,17, 19,21] have suggested that, while one hydrogen bond is formed upon adsorption on isolated silanol groups, two hydrogen bonds are formed when lone-pair electrons of the carbonyl oxygen interact with adjacent hydroxyl groups on the surface of silica. These interactions perturb the infrared bands associated with O–H and C=O stretching vibrations, thereby causing their shift to lower wavenumbers by 200–400 and 20–50 cm^{-1}, respectively. Finally, Hertl and Hair [7] have used their spectroscopic studies to estimate that isosteric heats for interactions of acetaldehyde and acetone with isolated hydroxyl groups on silica are 44 and 50 kJ/mol, respectively. Allian et al. [11], on the other hand, have estimated that the enthalpy change associated with the formation of hydrogen bonds between acetaldehyde and the surface of silica is 23 kJ/mol, and the corresponding standard entropy change was equal to 98 J/K mol.

In this report, we present results from experimental and theoretical investigations of the adsorption of acetaldehyde, methyl acetate, ethyl acetate, and methyl trifluoroacetate on silica. Silica is generally known to possess only weakly acidic properties; however, this study forms a basis for further studies of more acidic catalysts. Heat-flow microcalorimetry was used to measure the energies of interaction between the mentioned molecules and silica; temperature-programmed-desorption (TPD) spectroscopy was used to investigate the corresponding rates of desorption and to extract information about the changes in enthalpy and entropy associated with adsorption–desorption processes; Fourier-transform infrared spectroscopy (FTIR) was employed to study the nature of the surface species; and quantum-chemical calculations were performed on the basis of density-functional theory (DFT) to probe the potential energy surfaces for the interactions of carbonyl-containing molecules with silica. We will show that acetaldehyde, methyl acetate, ethyl acetate, and methyl trifluoroacetate adsorb on silica through the formation of hydrogen bonds with an average energy near 30 kJ/mol per bond, and the maximum rate of desorption generally occurs at temperatures between 325 and 400 K. The hydrogen bonds formed upon adsorption of these molecules involve the lone-pair electrons of the oxygen atom in the carbonyl group and hydroxyl groups on the surface of silica. At low coverages, esters can also form hydrogen bonds involving the alkoxy oxygen atom.

2. Methodology

Microcalorimetric measurements were performed using a Tian–Calvet, heat-flow microcalorimeter (Seteram C80) connected to a calibrated dosing system equipped with a capacitance manometer (Baratron, MKS). A detailed description of the apparatus and techniques may be found elsewhere [22,23]. Prior to each experiment, 500–600 mg of Cab–O–Sil (~380 m^2/g) was outgassed in vacuum (~1 mPa) for 2 h at 600 K and subsequently cooled to room temperature. The calorimetric cells were then placed in the isothermal block of the calorimeter, and measurements were initiated after the cells had equilibrated with the calorimeter at 300 K (typically overnight). Acetaldehyde (99.5%), methyl acetate (99.5%), ethyl acetate (99.5%), and methyl trifluoroacetate (99%) were purchased from Aldrich Chemicals and purified by performing freeze–pump–thaw cycles before each experiment.

Temperature-programmed-desorption studies were conducted using a Pyrex™ down-flow cell attached to a stainless-steel apparatus equipped with mass-flow controllers (Hastings) and a quadrupole mass spectrometer. The spectrometer consisted of a Quad 250B residual-gas analyzer (Electronic Associates) equipped with an electron-multiplier detector. The ionizing filament of the mass spectrometer was operated at pressures near 1 mPa, an electron energy of 70 eV, and an emission current of 150 μA. Helium (Liquid Carbonic) was used as a carrier gas and it was purified by flowing through copper turnings at 423 K followed by a bed of activated molecular sieves (13 X) at 77 K. Oxygen was used during the calcination of the samples and it was purified by flowing through a bed of activated molecular sieves at room temperature. Prior to TPD measurements, a sample of Cab–O–Sil was pretreated for 2 h in a stream of 20% oxygen in helium at 600 K. Afterwards, silica was saturated with the adsorbate, followed by purging of the TPD cell with flowing helium for 1 h at room temperature. Subsequently, the sample was heated to 600 K in a flow of helium at a rate of 10 K/min. The evolution of acetaldehyde, methyl acetate, ethyl acetate, and methyl trifluoroacetate was detected by monitoring signals at 29, 43, 43, and 15 amu/e, respectively. The amount of silica used in our studies varied between 34 and 160 mg while the flowrates of helium ranged from 35 to 120 cm^3/min.

Infrared spectra were collected at room temperature using a Mattson Galaxy 5020, FTIR spectrometer with a resolution of 2 cm^{-1}. Samples of Cab–O–Sil (10–30 mg) were pressed into self-supporting wafers ($\sim$ 12 mm in diameter) at a pressure of $\sim$ 60 MPa. Prior to spectroscopic measurements, the samples were outgassed in vacuum for 2 h at 600 K inside a cell equipped with CaF_2 windows. After collecting the spectrum for silica, a specific pressure of each adsorbate molecule was admitted into the cell, and spectra of the adsorbate on silica were collected. To investigate the reversibility of the adsorption processes, spectra were collected after outgassing overnight at room temperature and after outgassing for 2 h at 573 K.

Quantum-chemical calculations were performed on the basis of DFT, using the three-parameter functional B3LYP [24] along with the 6-31 + G* basis set [25]. Detailed information about the theory can be found elsewhere [26,27]. The calculations were performed using the software package Gaussian 94® [28] on DEC-alpha computers. Structural parameters were determined by optimizing to stationary points on the potential energy surface (PES) of the corresponding stoichiometry using the Berny algorithm and redundant internal coordinates [29]. For computational simplicity, hydrogen-terminated silanol groups were chosen to model the surface of silica. These models have been shown to be adequate for the quantitative description of interactions between oxygen-containing organic compounds and hydroxyl groups on silica [30–32]. Optimization criteria consisted of maximum and root-mean-squared forces of less than 22 and 15 J/mol pm, respectively. The molecular structures resulting from optimizations were classified as local minima on the PES by calculating the Hessian (force-constant) matrix analytically and ensuring that all its eigenvalues were positive. Vibrational frequencies obtained from analyses of force constants were used further without scaling to estimate thermochemical properties of the clusters at 298 K.

3. Results and discussion

3.1. Microcalorimetric and TPD measurements

Microcalorimetric data for the adsorption of acetaldehyde, methyl acetate, ethyl acetate, and methyl trifluoroacetate on silica at 300 K are shown in Fig. 1 in the form of differential heat of adsorption vs. surface coverage. For convenience, differential heats of adsorption have been defined as the negative of the differential changes in enthalpy associated with adsorption

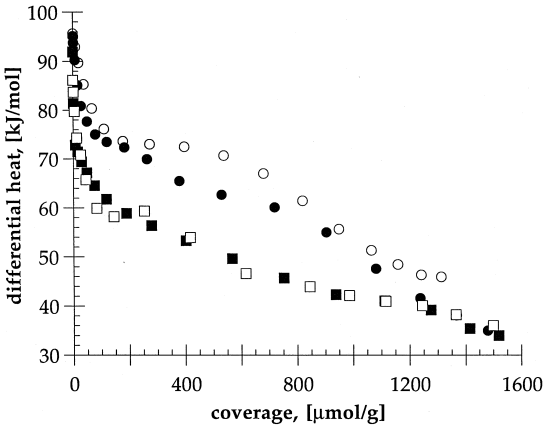

Fig. 1. Differential heat vs. surface coverage for the adsorption of acetaldehyde (□), methyl acetate (●), ethyl acetate (○), and methyl trifluoroacetate (■) on silica at 300 K.

processes. The initial heats for the adsorption of acetaldehyde, methyl acetate, ethyl acetate, and methyl trifluoroacetate on silica are 86, 95, 96, and 92 (± 5) kJ/mol, respectively. As the adsorbate coverage increases, differential heats of adsorption decrease monotonically, except for the case of ethyl acetate, until saturation of the surface at coverages near 1400 μmol/g. For ethyl acetate, the heat of adsorption is approximately constant at 72 ± 4 kJ/mol for coverages from 100 to 600 μmol/g, and the heat of adsorption then decreases monotonically until saturation of the surface.

Temperature-programmed-desorption spectra are shown in Fig. 2, and these spectra were collected using 70 mg of silica and a helium flowrate of 75 cm^3/min. The temperature corresponding to the peak maximum and the full width at half of the maximum intensity are listed in Table 1. Under these conditions, methyl and ethyl acetate desorb at a maximum rate near 376 K, and this peak temperature is 20 and 30 K higher than that for acetaldehyde and methyl trifluoroacetate, respectively. The peak widths for the desorption of methyl and ethyl acetate are also significantly broader than those for acetaldehyde and methyl trifluoroacetate. The shoulder observed at 410 K in the desorption spectrum of acetaldehyde can be assigned, as discussed later, to the presence of oligomers on

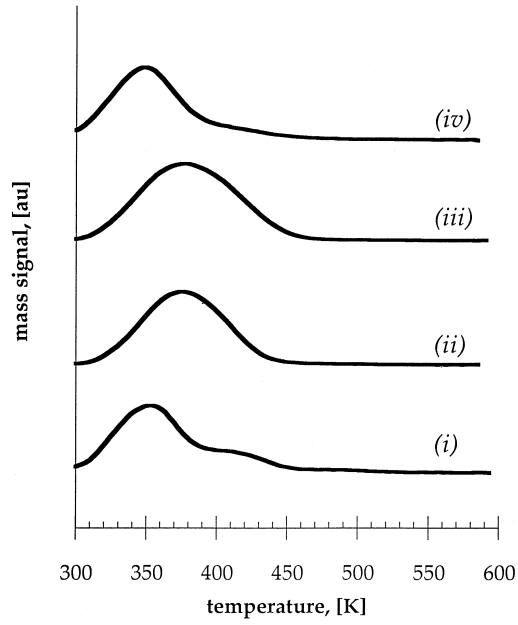

Fig. 2. Spectra for the temperature-programmed desorption from silica of (i) acetaldehyde, (ii) methyl acetate, (iii) ethyl acetate, and (iv) methyl trifluoroacetate using 70 mg of silica, a helium flowrate of 75 cm^3/min, and a heating rate of 10 K/min.

the surface. It can be concluded on the basis of thermal-desorption and microcalorimetric data that methyl and ethyl acetate exhibit nearly equal adsorption–desorption characteristics, and these properties are significantly different from those of acetaldehyde and methyl trifluoroacetate.

To extract the changes in enthalpy and entropy associated with the desorption of ethyl

Table 1
Maximum temperature (T_m) and full-width-at-half-maximum (FWHM) of the main peaks observed in Fig. 2 from the temperature-programmed desorption of carbonyl-containing compounds on silica

Adsorbate	T_m [K]	FWHM [K]	ΔH [kJ/mol]	$\Delta S°$ [J/K mol]
Acetaldehyde[a]	354	45	–	–
Methyl acetate	375	65	–	–
Ethyl acetate	378	79	65 ± 2	107 ± 5
Methyl trifluoroacetate	348	42	50 ± 4	89 ± 10

[a]A shoulder is also observed at 410 K in spectrum 3*i*.
Changes in enthalpy and entropy associated with the desorption of the adsorbates listed herein were obtained by the method shown in Fig. 3.

acetate and methyl trifluoroacetate from silica, TPD spectra were collected by varying the flowrate of the carrier gas from 35 to 75 to 120 cm^3/min. Results from these experiments are plotted in Fig. 3 in the form of $2\ln(T_m) - \ln(W/F)$ vs. $1/T_m$, where T_m is temperature corresponding to the maximum rate of desorption, W is the mass of the catalyst in grams, and F is the flowrate of the carrier gas, in cm^3/min, measured at room temperature. Assuming that adsorption–desorption processes are quasi-equilibrated during the TPD experiments, the slope of the resulting line is equal to $-\Delta H/R$. The intercept is given by $\ln\{-A_0T_0\beta\Delta H(1-\theta_m)^2/P_0\} + \Delta S^\circ/R$, where A_0 is the site density in mol/g, T_0 is 298 K, β is the heating rate in K/min, P_0 is the standard-state pressure (10^5 Pa), and θ_m is the fractional surface coverage at the temperature T_m. Estimates of θ_m were obtained by following the methods of Cvetanovic and Amenomiya [33], and site densities were determined by extrapolating coverages from adsorption isotherms to zero pressure. As shown in Table 1, the enthalpy and entropy changes associated with the desorption of ethyl acetate from silica are 65 ± 2 kJ/mol and 107 ± 5 J/K mol, whereas these values are 50 ± 4 kJ/mol and 89 ± 10 J/K mol in the case of methyl trifluoroacetate. The heat of desorption of ethyl acetate obtained from TPD corresponds well with the constant heat at 72 ± 4 kJ/mol observed in the differential-heat plot (Fig. 1) associated with the adsorption of ethyl acetate on silica.

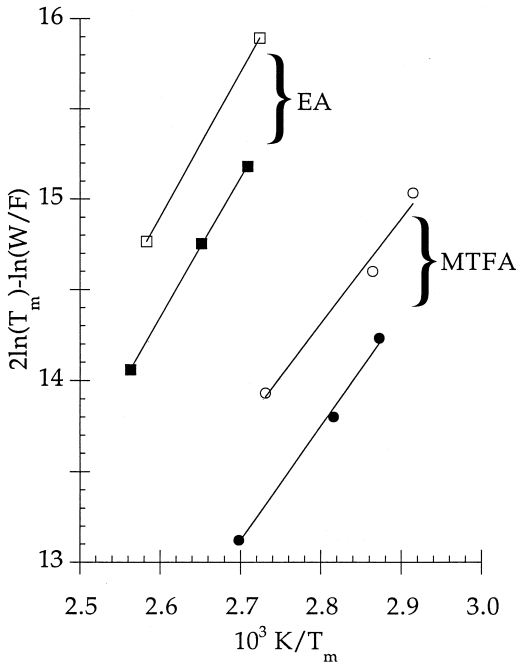

Fig. 3. Plots used for the determination of changes in enthalpy and entropy associated with the adsorption of ethyl acetate (□, ■) and methyl trifluoroacetate (○, ●). Analyses comprised five and six data points, respectively, for ethyl acetate and methyl trifluoroacetate. Experimental conditions consisted of a heating rate of 10 K/min; helium flowrates of 35, 75, and 120 cm^3/min (measured at room temperature); and sample sizes corresponding to 34 (□), 70 (■, ○), and 160 (●) mg of silica.

The adsorption of aldehydes and esters on silica involves the formation of hydrogen bonds. On the basis of the heat of 23–44 kJ/mol reported elsewhere [7,11] for the adsorption of acetaldehyde on isolated silanol groups, our microcalorimetric and TPD results suggest the formation of multiple hydrogen bonds between the molecules in this study and the surface of silica. Multiple hydrogen bonds are formed with geminal and vicinal hydroxyl groups present on samples of silica that have been pretreated at temperatures below 773 K [34–37], which is the situation in this study. Rochester and coworkers [16,17,19,21] have suggested that, while one hydrogen bond is formed upon adsorption on isolated silanol groups, two bonds are formed when lone-pair electrons on the carbonyl oxygen interact with adjacent hydroxyl groups on silica. Therefore, the heats of adsorption of ethyl acetate and methyl acetate assessed from thermal-desorption data, and from microcalorimetric data at coverages greater than 100 μmol/g, may be tentatively assigned to species bound to silica by two hydrogen bonds. Accordingly, the hydrogen-bond strengths for these esters on silica are both 34 ± 4 kJ/mol per bond. In contrast, the hydrogen-bond strengths for acetaldehyde and methyl trifluoroacetate on silica appear both to be 27 ± 4 kJ/mol. Replacement of the alkoxy group by a hydrogen

atom, as in the case of acetaldehyde vs. methyl and ethyl acetate, results in a decrease in the ability of the carbonyl oxygen to donate electron density to the hydrogen atom in the hydroxyl group. Similarly, fluorination of the acyl fragment of the ester, as in the case of methyl trifluoroacetate vs. methyl acetate, results in a decrease in the electron donation ability of the carbonyl oxygen because of the electron-withdrawing nature of perfluoroalkyl groups. It should be noted that since there are also two lone pairs of electrons on the alkoxy oxygen of esters, more than two hydrogen bonds could be formed between these molecules and silica, and thereby result in the relatively high heats of adsorption observed at coverages below 100 μmol/g. This possibility will be explored later by means of DFT calculations.

Changes in entropy associated with adsorption processes provide information about the mobility of the corresponding surface species. If it is assumed that one degree of translational freedom is lost upon adsorption of the esters on silica, as in the case of a fairly mobile adsorbate, then the corresponding changes in entropy would be near -92 J/K mol, for a total site concentration of 10^{15} cm^{-2}. This value corresponds roughly to the entropies of adsorption listed in Table 1. Therefore, the surface species resulting from the adsorption of acetaldehyde and the esters considered in this study on silica are relatively mobile.

3.2. Spectroscopic measurements

Infrared absorption spectra for acetaldehyde, methyl acetate, ethyl acetate, and methyl trifluoroacetate on silica are shown in Fig. 4. The bands in this figure are listed in Tables 2–5,

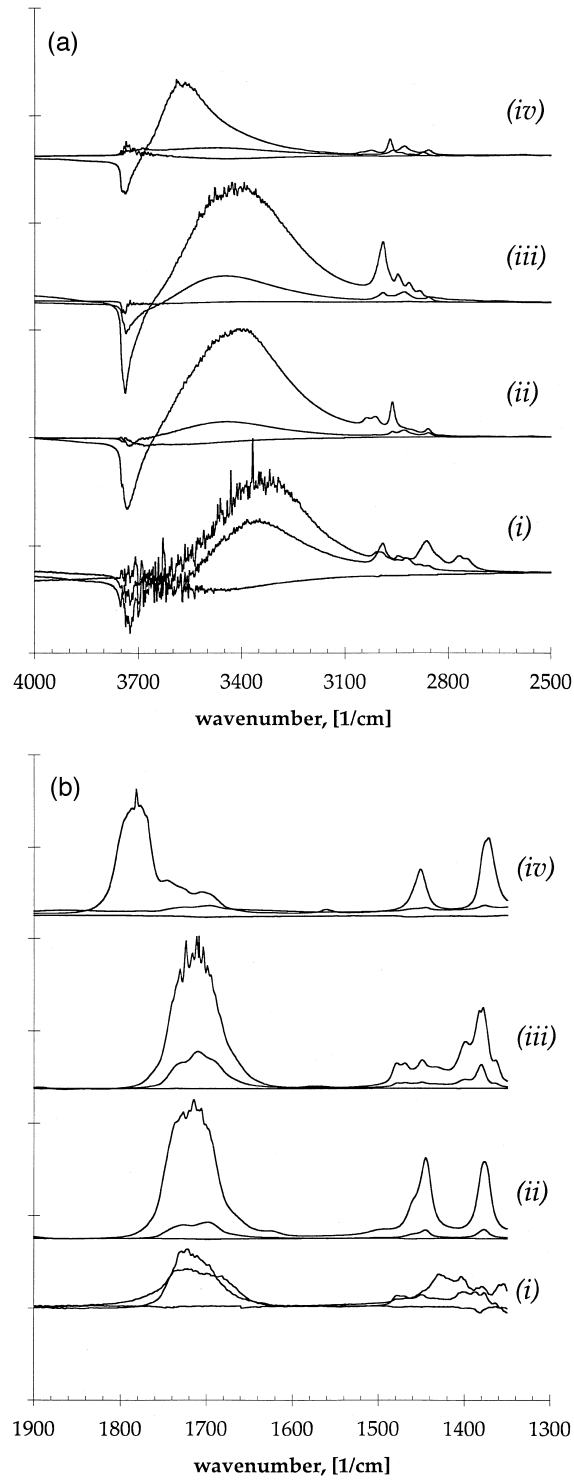

Fig. 4. FTIR difference spectra for wavenumber regions (a) from 4000 to 2500 cm^{-1} and (b) from 1900 to 1400 cm^{-1} associated with (i) 650 μmol/g of acetaldehyde, (ii) 610 μmol/g of methyl acetate, (iii) 630 μmol/g of acethyl acetate, and (iv) 610 μmol/g of methyl trifluoroacetate adsorbed on silica at room temperature. The superimposed spectra correspond to each sample after outgassing in vacuum overnight at room temperature and after outgassing for 2 h at 573 K. Vertical axes in (a) and (b) are both divided in 5.0 absorbance units.

Table 2
Wavenumbers (cm^{-1}) for some of the fundamental modes of vibration of acetaldehyde in the gas phase (C_s point group) and adsorbed on silica

description	experimental			dft predictions		
	gas	650 μmol/g 4(*ai*, *bi*)	evacuated 4(*ai*, *bi*)	gas	5(a)	5(b)
$\upsilon_{as}'(CH_3)$	3024 (R)	3008		3043	3049	3051
	2996 (P)	2992	2988			
$\upsilon_{as}''(CH_3)$	2964	2948	2944	2982	2984	2985
$\upsilon_s(CH_3)$	2923	2922	2914	2929	2932	2933
	2840 (R)		2880			
	2822 (Q)	2862	2856	2808	2861	2878
υ(CH)	2804 (P)					
	2736 (R)	2766				
	2704 (P)	2742				
	1763 (R)					
υ(C=O)	1749 (Q)	1722	1724	1751	1730	1725
	1735 (P)		1688			
$\delta_{as}''(CH_3)$	1436	1478	1478	1437	1435	1432
		1468	1470			
$\delta_{as}'(CH_3)$	1430	1448	1448	1429	1427	1428
		1430				
δ′(CH)	1395	1404	1406	1382	1389	1388
		1398	1400			
		1384	1388			
$\delta_s(CH_3)$	1353	1378	1376	1350	1353	1357
		1360	1364			
		1352	1356			
υ(OH)	3680	3336	3360		3445	3560
						3536

Columns are identified by the corresponding figure number in this report. DFT predictions have been scaled by a factor of 0.964 to obtain the best match between theoretical and experimental vibrational spectra for gaseous acetaldehyde. The experimental spectrum for gaseous acetaldehyde was taken from Refs. [6,42,43].

along with assigned vibrational modes, literature data, and theoretical predictions from this work. These spectroscopic measurements consisted first of dosing a specific amount of each molecule onto silica at room temperature to achieve a surface coverage from 600 to 650 μmol/g, followed by collection of the spectra. The pressures of acetaldehyde, methyl acetate, ethyl acetate, and methyl trifluoroacetate used were 276, 48, 58, and 554 Pa, respectively. Afterwards, each sample was evacuated overnight at room temperature to investigate the reversibility of the adsorption processes. Assuming that the decrease in the intensity of the υ(OH) bands in Fig. 4 is proportional to the adsorbate coverage, we conclude that roughly 370, 90, 150, and 65 μmol/g of acetaldehyde, methyl acetate, ethyl acetate, and methyl trifluoroacetate, respectively, remained on silica after evacuation at room temperature. Further evacuation at 573 K resulted in the complete removal of the adsorbates from the surface of silica.

The adsorption of the carbonyl-containing molecules in this study resulted in the simultaneous perturbation of O–H and C=O stretching bands, indicating interactions between hydroxyl

Table 3
Wavenumbers (cm^{-1}) for some of the fundamental modes of vibration of methyl acetate in the gas phase (C_s point group) and adsorbed on silica

description	experimental			dft predictions		
	gas	610 μmol/g 4(*aii, bii*)	evacuated 4(*aii, bii*)	gas	6(a)	6(b)
$\upsilon_{as}'(OCH_3)$	(3040)	(3036)	(3036)	3092	3100	3110
$\upsilon_{as}'(CCH_3)$	(3040)	(3036)	(3036)	3088	3092	3090
$\upsilon_{as}''(OCH_3)$	(3000)	(3012)	(3012)	3062	3071	3083
$\upsilon_{as}''(CCH_3)$	(3000)	(3012)	(3012)	3042	3043	3053
$\upsilon_s'(OCH_3)$	2971 (R) 2964 (Q) 2955 (P)	2962	2982 2960	2989	2995	3002
$\upsilon_s'(CCH_3)$	2940	2928	2928	2983	2983	2983
$2\delta_{as}''(CCH_3)$	2908	2904				
$2\delta_{as}'(CCH_3)$	2862	2858	2874 2856			
$\upsilon(C{=}O)$	1775 (R) 1769 1760 (P)	1730 1716 1700	1728 1698	1753	1718	1698
$\delta_{as}'(OCH_3)$	1467	1498	1500	1475	1473	1473
$\delta_{as}''(OCH_3)$	1459	1460	1458	1464	1466	1472
$\delta_{as}''(CCH_3)$	1446	1446	1444	1458	1461	1462
$\delta_{as}'(CCH_3)$	(1439)			1453	1453	1453
$\delta_s'(OCH_3)$	(1439)			1445	1448	1445
$\delta_s'(CCH_3)$	1378	1376	1376	1381	1389	1389
$\upsilon(OH)$	3742 3690	3410	3444		3462	3570, 3534

Columns are identified by the corresponding figure number in this report. DFT predictions have been scaled by a factor of 0.972. The experimental spectrum for gaseous methyl acetate was taken from Ref. [44].

groups on the surface of silica and the carbonyl oxygen in the adsorbed molecules. In particular, the υ(OH) band shifted to lower wavenumbers by 344, 280, 286, and 130 cm^{-1} upon adsorption of acetaldehyde, methyl acetate, ethyl acetate, and methyl trifluoroacetate, respectively, whereas the υ(C=O) bands shifted to lower wavenumbers by 25–80 cm^{-1} for the nonfluorinated compounds and by as much as 114 cm^{-1} for methyl trifluoroacetate. As shown in Fig. 4b, the υ(C=O) bands appeared rather broad, and sometimes exhibited several maxima, thus indicating the existence of several adsorbate states involving a different number of hydrogen bonds, or perhaps different environments. This interpretation is consistent with interactions involving the linkage of carbonyl-containing molecules via two hydrogen bonds to a pair of adjacent silanol groups.

It can be seen in Tables 2–5 that the C–H stretching and bending modes of vibration were perturbed upon adsorption to a smaller extent than were the υ(C=O) and υ(OH) bands. In particular, most of the perturbed bands shifted to higher wavenumbers by 10–30 cm^{-1}. However, some of the bands associated with vibrations involving C–H bonds shifted to lower wavenumbers. This observation supports the coexistence of various types of surface interactions. As shown in Fig. 4a for acetaldehyde adsorbed on silica, several bands appeared in the C–H stretching region of the spectrum collected after evacuating the sample at room temperature that were not observable prior to this

Table 4
Wavenumbers (cm^{-1}) for some of the fundamental modes of vibration of ethyl acetate in the gas phase (C_s point group) and adsorbed on silica

description	experimental			dft predictions		
	gas	630 μmol/g 4(*aiii*,*biii*)	evacuated 4(*aiii*,*biii*)	gas	like 6(a)	like 6(b)
$\upsilon_{as}'(CCH_3)$				3060	3064	3061
$\upsilon_{as}''(OCH_3)$				3021	3026	3034
$\upsilon_{as}''(CCH_3)$	3008			3014	3016	3026
$\upsilon_{as}'(OCH_3)$	2996			3008	3011	3016
$\upsilon_{as}''(CH_2)$	2988	(2988)	(2988)	2996	3003	3011
$\upsilon_{s}'(CH_2)$	2982	(2988)	(2988)	2961	2968	2975
$\upsilon_{s}'(CCH_3)$	2956			2956	2957	2956
$\upsilon_{s}'(OCH_3)$	2948	2946		2943	2946	2949
$2\delta'(CH_2)$	2924		2930			
$2\delta_{as}''(OCH_3)$	2914	2912				
$2\delta_{as}''(CCH_3)$		2882	2878 2856			
$\upsilon(C{=}O)$	1770 (R) 1760 (P)	1680-1740	1694, 1710, 1730	1733	1697	1675
$\delta'(CH_2)$	1464	1478	1478	1480	1479	1477
$\delta_{as}'(OCH_3)$	liquid: 1466	1468	1470	1464	1464	1464
$\delta_{as}''(OCH_3)$	liquid: 1455			1455	1455	1456
$\delta_{as}''(CCH_3)$	liquid: 1448	1448	1450	1446	1448	1448
$\delta_{as}'(CCH_3)$	liquid: 1429	1430		1440	1441	1440
$\delta_{s}'(OCH_3)$	1384	1398 1382	1400	1394	1396	1398
$\delta_{s}'(CCH_3)$	1377	1378	1380	1372	1380	1379
$\rho_{r}'(CH_2)$	1371	1364	1364	1356	1359	1362
$\upsilon(OH)$	3740 3696	3410	3448	—	3423	3533, 3495

Columns are identified by the corresponding figure number in this report. DFT predictions have been scaled by a factor of 0.964. The experimental spectrum for gaseous ethyl acetate was collected during our studies and combined with that in Refs. [45,46].

treatment. Furthermore, $\upsilon(C{=}O)$ appeared as a peak near 1722 cm^{-1} in the spectrum collected prior to evacuation, while a second peak appeared at 1688 cm^{-1} after the evacuation procedure. These results are in good agreement with previous reports [1,6], and they have been interpreted in terms of the surface oligomerization of acetaldehyde molecules to eventually yield crotonaldehyde via aldol-condensation reactions. These oligomerization processes may be responsible for the relatively high heats of acetaldehyde adsorption obtained microcalorimetrically since acetaldehyde can form at most two hydrogen bonds with silanol groups, and thereby liberate less than 70 kJ/mol.

3.3. DFT calculations

Various clusters were considered that involve interactions between hydrogen-terminated silanol groups and each adsorbate molecule to study the adsorption of acetaldehyde, methyl acetate, ethyl acetate, and methyl trifluoroacetate on silica. These clusters represent adsorption of the molecules on isolated and vicinal silanol groups. The optimized structures of these

Table 5
Wavenumbers (cm^{-1}) for some of the fundamental modes of vibration of methyl trifluoroacetate in the gas phase and adsorbed on silica

description	experimental			dft predictions		
	gas	610 μmol/g 4(*aiv,biv*)	evacuated 4(*aiv,biv*)	gas	like 6(a)	like 6(b)
υ(C=O)+υ_{as}'(CF_3)	3052	3052				
υ_{as}'(CH_3)	3022	3024		3061	3068	3074
υ_{as}''(CH_3)	2980	2970	2960	3027	3036	3046
υ_{s}'(CH_3)	2920	2932	2926	2950	2955	2960
$2\delta_{as}$(CH_3)	2875	2908 2870	2856			
υ_{s}'(CF_3)+υ(CC)	1990		1988			
υ(C=O)	1818	1784 1704	1776 1698	1762	1744	1727
υ_{s}'(CF_3)+δ_{as}'(CF_3)	1746	1746	1728			
$2\rho_{w}''$(C=O)	1565	1560				
δ_{as}'(CH_3)	1470			1446	1444	1447
δ_{as}''(CH_3)	1458	1452	1460 1446	1441	1442	1444
δ_{s}'(CH_3)	1370	1374	1378	1424	1426	1427
υ(OH)	3742 3700	3570	3484		3568	3585, 3554

Columns are identified by the corresponding figure number in this report. DFT predictions have been scaled by a factor of 0.956. The experimental spectrum for gaseous methyl trifluoroacetate was taken from Refs. [47–49].

clusters are shown in Figs. 5–7, the corresponding energetic information is listed in Table 6, and structural parameters are listed in Tables 7 and 8.

The adsorption of carbonyl-containing compounds on silica is known to proceed via formation of hydrogen bonds between the lone-pair orbital on the carbonyl oxygen and hydroxyl groups on the oxide surface [1,5–21]. The involvement of the carbonyl oxygen in hydrogen-bonding interactions with the surface can be understood in terms of the highest-occupied molecular orbital (HOMO) of carboxylic acids and their derivatives. These molecules can be denoted collectively by RCOX, where R represents an alkyl group and X is either OH, OR′, or NR_2. On the basis of photoelectron spectra, Sweigart and Turner [38] have concluded that the lone-pair orbital n_0 on the carbonyl oxygen and the approximately nonbonding, antisymmetric π_2 orbital are the two occupied molecular orbitals of highest energy, and they have similar ionization potentials. The latter orbital arises mainly from the combination of p orbitals on the O and X species within the COX fragment of the molecule. If the conjugation between X

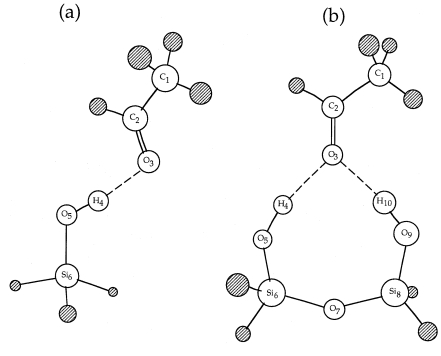

Fig. 5. Optimized clusters used to study the adsorption of acetyldehyde on (a) a hydrogen-terminated, isolated silanol group and (b) on hydrogen-terminated, vicinal silanol groups. The corresponding structural parameters are listed in Table 7.

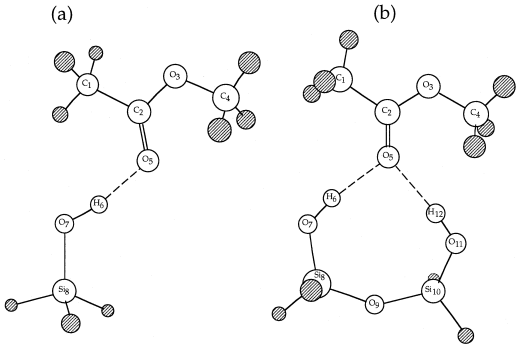

Fig. 6. Optimized clusters used to study the adsorption of methyl acetate on (a) a hydrogen-terminated, isolated silanol group and (b) on hydrogen-terminated, vicinal silanol groups. The corresponding structural parameters are listed in Table 8. The cases of ethyl acetate and methyl trifluoroacetate are analogous, and their structural parameters are also listed in Table 8, following the nomenclature used herein and Fig. 7.

and the carbonyl group were removed, then the π_2 orbital would correspond to the lone-pair orbital in the X group. These conclusions are supported by our DFT calculations.

The adsorption of acetaldehyde on isolated and vicinal silanol groups is represented by the optimized clusters in Fig. 5a and b, respectively. The corresponding structural parameters are listed in Table 7. As shown in Table 6, the changes in energy and entropy associated with interactions of lone-pair electrons on the carbonyl group of acetaldehyde with a single silanol group are predicted to be 29 kJ/mol and 111 J/K mol. These results are in agreement with the values of 23 kJ/mol and 98 J/K mol reported by Allian et al. [11]. The changes in energy and entropy predicted for the adsorption of acetaldehyde on vicinal silanol groups are 39 kJ/mol and 144 J/K mol. Even though the former value is reasonable, the predicted change in entropy appears to be overestimated in comparison to the values determined from thermal-desorption data. In any case, these calculations support the conclusion that the strength of the hydrogen bonds between acetaldehyde and silanol groups is near 25 kJ/mol, and that the high heats determined microcalorimetrically at low coverages probably correspond to competing surface processes such as the oligomerization of acetaldehyde on silica.

Gaseous acetaldehyde is predicted to belong to the C_s point group. The lengths of C_1–C_2, C_2=O_3, and C–H bonds are predicted to be 151, 121, and 109–111 pm, respectively, while the C_1–C_2–O_3 angle is 124.7°. Acetaldehyde retains a local C_s symmetry upon interactions with a single silanol group, as can be seen in Fig. 5a, but its structure is slightly perturbed. The length of the O_3–H_4 hydrogen bond formed is estimated to be 185 pm, and this bond is almost linear with respect to the hydroxyl group, as indicated by the O_3–H_4–O_5 angle of 166.7°. The C_2=O_3–H_4 angle is 112.3°. These results are in agreement with quantum-chemical studies by Ugliengo et al. [10] of the adsorption of formaldehyde on isolated silanol groups, and also with the description of hydrogen-bonded complexes by Legon and Millen [39,40], according to whom O–H–O and C=O–H angles are expected to be 180° and 120°, respectively, because the oxygen atom in acetaldehyde is sp^2-hybridized. When bonding with vicinal

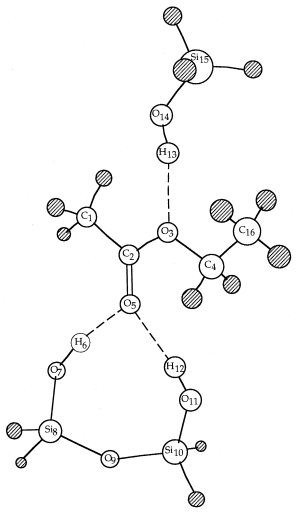

Fig. 7. Optimized cluster used to study the adsorption of ethyl acetate on a site comprising three silanol groups. The corresponding structural parameters are listed in Table 8. The cases of methyl acetate and methyl trifluoroacetate are analogous, and their structural parameters are also listed in Table 8, following the nomenclature used herein and in Fig. 6.

Table 6
Energetics predicted for the adsorption of acetaldehyde, methyl acetate, ethyl acetate, and methyl trifluoroacetate on silica at 298 K

	$-\Delta E^{a}$ [kJ/mol]	$-\Delta H$ [kJ/mol]	$-\Delta S^{\circ}$ [J/K mol]
Acetaldehyde			
$AcH + H_3SiOH \rightarrow AcH–HOSiH_3$ (**5a**)	29	22	110
$AcH + H_4Si_2O(OH)_2 \rightarrow AcH–(OH)_2OSi_2H_4$ (**5b**)	39	31	144
Methyl acetate			
$MA + H_3SiOH \rightarrow MA–HOSiH_3$ (**6a**)	32	25	115
$MA + H_4Si_2O(OH)_2 \rightarrow MA–(OH)_2OSi_2H_4$ (**6b**)	45	36	153
$MA + H_4Si_2O(OH)_2 + H_3SiOH \rightarrow H_3SiOH–MA–(OH)_2OSi_2H_4$	59	–	–
Ethyl acetate			
$EA + H_3SiOH \rightarrow EA–HOSiH_3$	33	26	111
$EA + H_4Si_2O(OH)_2 \rightarrow EA–(OH)_2OSi_2H_4$	46	38	149
$EA + H_4Si_2O(OH)_2 + H_3SiOH \rightarrow H_3SiOH–EA–(OH)_2OSi_2H_4$ (**7**)	61	–	–
Methyl trifluoroacetate			
$MTFA + H_3SiOH \rightarrow MTFA–HOSiH_3$	20	13	111
$MTFA + H_4Si_2O(OH)_2 \rightarrow MTFA–(OH)_2OSi_2H_4$	30	22	155
$MTFA + H_4Si_2O(OH)_2 + H_3SiOH \rightarrow H_3SiOH–MTFA–(OH)_2OSi_2H_4$	43	–	–

[a] Values in this column have not been corrected for changes in zero-point vibrational energies.

silanol groups, acetaldehyde appears to retain a local C_s symmetry, and its structure is similar to that on a single hydroxyl group; however, the two hydrogen bonds formed in this case are significantly longer by $\sim$10 pm. In all cases, silanol groups are also perturbed slightly, causing them to stretch by $\sim$1 pm.

The adsorption of methyl acetate on isolated and vicinal silanol groups is represented by the optimized clusters in Fig. 6a and b, respectively. Figures corresponding to the cases of ethyl acetate and methyl trifluoroacetate adsorbed on isolated and vicinal silanol groups are not included because they are analogous to those shown in Fig. 6; however, their structural parameters are listed in Table 8. As shown in Table 6, the changes in energy associated with interactions of methyl and ethyl acetate with a single silanol group are predicted to be approximately 32 kJ/mol, while the energy change for methyl trifluoroacetate adsorption is predicted to be near 20 kJ/mol. Changes in entropy are predicted to be from 111 to 115 J/K mol. These results are consistent with our thermal-desorption and microcalorimetric data, which suggest that methyl trifluoroacetate is bound less strongly than methyl and ethyl acetate on silanol groups. The changes in energy associated with adsorption of methyl and ethyl acetate on vicinal silanol groups are predicted to be 46 kJ/mol, and the energy change for methyl trifluoroacetate adsorption is 30 kJ/mol. Changes in entropy are predicted to be from 144 to 155 J/K mol. These heats of interaction between the carbonyl group in esters and vicinal silanol groups seem to be underestimated when compared to our thermal-desorption data. The error associated with the description of the adsorption characteristics of methyl trifluoroacetate is most likely caused by the need to use triple-split basis sets when modelling fluorinated compounds [41]. More generally, uncertainties in our calculations are caused by basis-set superposition errors (BSSE) [50] and by the intrinsic inability of generalized-gradient-approximation (GGA) methods to account for weak chemical interactions, namely van der Waals interactions [26]. It has been shown [51] that the use of large basis sets analogous to 6-31 + G* introduces an error lower than 5 kJ/mol for the simulation of hydrogen-bonding interactions. On the other hand, usage of GGA methods can result in

Table 7
Structural parameters for optimized clusters of acetaldehyde in the gaseous phase and interacting with one and two silanol groups

	Gas	**5a**	**5b**
Distances (pm)			
C_1C_2	151	150	150
C_2O_3	121	122	122
O_3H_4	–	185	197
H_4O_5	–	98	98
O_5Si_6	–	166	166
Si_6O_7	–	–	165
O_7Si_8	–	–	165
Si_8O_9	–	–	166
O_9H_{10}	–	–	98
$H_{10}O_3$	–	–	195
HC_1	109, 110, 110	109, 110, 110	109, 110, 110
HC_2	111	111	111
HSi_6	–	148–149	148–149
HSi_8	–	–	148–149
Angles [°]			
$C_1C_2O_3$	124.7	124.0	124.5
$C_2O_3H_4$	–	112.3	133.0
$O_3H_4O_5$	–	166.7	165.4
$H_4O_5Si_6$	–	119.0	117.7
$O_5Si_6O_7$	–	–	112.4
$Si_6O_7Si_8$	–	–	150.3
$O_7Si_8O_9$	–	–	112.2
$Si_8O_9H_{10}$	–	–	117.2
$O_9H_{10}O_3$	–	–	168.4
HC_1H	106.7, 110, 110	106.6, 110, 110	106.5, 110, 110
HC_2C1	115.4	116.4	116.6
HSi_6H	–	107–110	111.5
HSi_8H	–	–	111.4

energies of interaction lower than accepted values by as much as 20 kJ/mol.

Gaseous methyl acetate, ethyl acetate, and methyl trifluoroacetate are predicted to belong to the C_s point group. These esters retain a local C_s symmetry when interacting with a single silanol group, as can be seen in Fig. 6a for the case of ethyl acetate, but their structures are slightly perturbed. The length of the O_5–H_6 hydrogen bond formed between methyl or ethyl acetate and a single silanol group is estimated to be 183 pm, whereas this bond is longer by 15 pm in the case of methyl trifluoroacetate, suggesting a weaker interaction. The hydrogen bond O_5–H_6 is almost linear in all cases with respect to the hydroxyl group: O_5–H_6–O_7 angles range from 168 to 171°. The C_2=O_5–H_6 angles are both ~119° in the cases of methyl and ethyl acetate, but greater by ~20° for methyl trifluoroacetate. These results are consistent with those presented above for acetaldehyde. When bonding with vicinal silanol groups, the esters do not retain any symmetry. The lengths of the two hydrogen bonds formed in these cases range from 185 to 194 pm.

Contributions to the energy of hydrogen bonds arise primarily from interactions caused by the transfer of electron density from the carbonyl oxygen to the hydrogen atom of the acidic species (the silanol group). These interactions can be investigated by following the Mulliken charges associated with the adsorbate and the silanol group(s). For instance, the charges transferred to the isolated silanol groups in Figs. 5a and 6a upon adsorption of acetaldehyde and methyl trifluoroacetate are calculated to be 0.021 e and 0.022 e, respectively. Similarly, when methyl acetate, ethyl acetate, and methyl trifluoroacetate adsorb on vicinal silanol groups, as in Fig. 6b, the extent of charge transfer to the hydroxyl groups is predicted to be 0.035 e, 0.053 e, and 0.039 e, respectively. Despite the fact that the absolute values of population analyses have very little meaning because they depend strongly on the partitioning scheme, it should be noted that a net flow of electronic charge is predicted from the carbonyl-containing adsorbate to the hydroxyl groups with which they bond.

Vibrational spectra predicted for the probe molecules of this study adsorbed on one and two silanol groups are included in Tables 2–5. As observed experimentally, the bands associated with υ(C=O) and υ(OH) modes of the molecule and silanol groups, respectively, are affected most significantly. The cases of methyl and ethyl acetate on a single silanol group are very similar: υ(C=O) and υ(OH) bands are predicted to shift to lower wavenumbers by 35–36 and 251–260 cm^{-1}, respectively; on vicinal silanol groups, these shifts are 55–58 and 137–182 cm^{-1}. Similarly, the υ(C=O) bands corresponding to acetaldehyde and methyl tri-

Table 8
Structural parameters for optimized clusters of methyl acetate, ethyl acetate, and methyl trifluoroacetate in the gaseous phase and interacting with one, two, and three silanol groups

	Methyl acetate				Ethyl acetate				Methyl trifluoroacetate			
	Gas	**6(a)**	**6(b)**	Like **7**	Gas	Like **6(a)**	Like **6(b)**	**7**	Gas	Like **6(a)**	Like **6(b)**	Like **7**
Distances (pm)												
C_1C_2	151	151	150	150	151	151	151	150	155	155	155	155
C_2O_3	135	134	133	135	135	134	133	134	133	132	131	131
O_3C_4	144	144	145	145	145	145	146	147	145	145	146	146
C_4C_{16}	–	–	–	–	152	152	152	152	–	–	–	–
C_2O_5	121	122	123	122	122	122	123	123	121	121	122	121
O_5H_6	–	183	190	192	–	183	190	191	–	197	208	208
H_6O_7	–	98	98	98	–	98	98	98	–	97	97	97
O_7Si_8	–	166	166	166	–	166	166	166	–	166	166	166
Si_8O_9	–	–	166	166	–	–	166	166	–	–	166	166
O_9Si_{10}	–	–	165	165	–	–	165	165	–	–	165	165
$Si_{10}O_{11}$	–	–	166	166	–	–	166	166	–	–	167	167
$O_{11}H_{12}$	–	–	98	97	–	–	98	98	–	–	97	97
$H_{12}O_5$	–	–	192	193	–	–	191	192	–	–	199	199
O_3H_{13}	–	–	–	199	–	–	–	201	–	–	–	225
$H_{13}O_{14}$	–	–	–	98	–	–	-	97	–	–	–	97
$O_{14}Si_{15}$	–	–	–	167	–	–	–	167	–	–	–	168
Angles, [°]												
$C_1C_2O_3$	111.2	112.0	112.8	113.0	111.2	112.2	113.0	113.2	109.6	110.3	110.5	110.8
$C_2O_3C_4$	116.0	116.6	117.6	117.4	116.5	147.0	118.0	117.6	116.0	116.5	117.6	118.0
$O_3C_4C_{16}$	–	–	–	–	107.6	107.5	107.4	107.8	–	–	–	–
$C_1C_2O_5$	125.6	125.5	124.2	124.9	125.4	125.3	123.8	124.6	123.2	123.0	122.2	121.7
$C_2O_5H_6$	–	118.7	127.7	128.5	–	119.2	127.2	128.4	–	139.0	136.4	136.0
$O_5H_6O_7$	–	169.0	169.7	169.4	–	170.8	170.0	169.6	–	168.2	156.3	158.0
$H_6O_7Si_8$	–	119.0	117.7	117.9	–	118.9	117.6	117.8	–	117.9	119.0	118.8
$O_7Si_8O_9$	–	–	112.3	112.2	–	–	112.2	112.2	–	–	112.2	112.0
$Si_8O_9Si_{10}$	–	–	148.2	148.4	–	–	147.7	148.0	–	-	145.6	148.7
$O_9Si_{10}O_{11}$	–	–	112.0	112.0	–	-	112.2	112.0	–	-	111.2	111.4
$Si_{10}O_{11}H_{12}$	–	–	117.4	117.7	–	–	117.3	117.3	–	–	116.5	117.2
$O_{11}H_{12}O_5$	–	–	171.3	171.4	–	–	171.3	171.0	–	–	163.8	163.8
$H_{12}O_5C_2$	–	–	139.5	139.8	–	-	139.3	139.7	–	-	134.0	134.8
$C_2O_3H_{13}$	–	–	–	119.3	–	–	-	118.9	–	–	–	136.3
$O_3H_{13}O_{14}$	–	–	–	161.3	–	–	–	159.7	–	–	–	126.4
$H_{13}O_{14}Si_{15}$	–	–	–	119.3	–	–	–	119.7	–	–	–	118.4

The HCH and FCF angles are predicted to be $109 \pm 2°$, while CH and CF distances are 133–135 and 109–110 pm, respectively.

fluoroacetate on one and two silanol groups are predicted to shift by 18–21 and 26–35 cm^{-1}, respectively. Moreover, while the shifts to lower wavenumbers of υ(OH) bands caused by acetaldehyde adsorption on one and two silanol groups are 238 and 117–141 cm^{-1}, respectively, shifts of the υ(OH) band caused by adsorption of methyl trifluoroacetate are predicted to be less than 100 cm^{-1}. The smaller υ(OH)-shifts predicted in the case of methyl trifluoroacetate are related to the weaker hydrogen bonds formed by this ester on silica, mainly caused by the electron-withdrawing effect of the perfluoromethyl group on the C=O bond.

In addition to the lone-pair electrons of the carbonyl oxygen, there are lone-pair electrons associated with the alkoxy oxygen in esters. In fact, the energy of the orbital containing the latter electrons is just below that of the HOMO. Therefore, it is possible to form hydrogen bonds involving the alkoxy oxygen in esters after the carbonyl oxygen is saturated, thus resulting in a

maximum of four hydrogen bonds per ester molecule. Nevertheless, the number of sites on the surface of silica capable of accommodating such a number of hydrogen bonds is expected to be limited.

The optimized structure of the clusters used to represent the adsorption of ethyl acetate on a surface site comprising three silanol groups is shown in Fig. 7. Figures corresponding to the cases of methyl acetate and methyl trifluoroacetate are not included because they are analogous to that shown in Fig. 7; however, their structural parameters are listed in Table 8. As shown in Table 6, the changes in energy associated with interactions of methyl and ethyl acetate with three silanol groups are predicted to be approximately 60 kJ/mol, while that for methyl trifluoroacetate adsorption is predicted to be 43 kJ/mol. While the latter value seems underestimated, the predicted heat of adsorption of methyl and ethyl acetate on three silanol groups is reasonable. Sources of error in our calculations are discussed above. Even though the hydrogen-bond strength of 20 kJ/mol per bond is lower than the values obtained from our microcalorimetric and TPD studies and from our calculations using a single silanol group, these results support the idea that the alkoxy oxygen can be involved in hydrogen bonding with the surface of silica. Therefore, the high heats of ester adsorption at coverages below 100 μmol/g may be related to the formation of more than two hydrogen bonds between the surface of silica and each ester. This conclusion is supported by our spectroscopic measurements since, as mentioned previously, the appearance of several υ(C=O) bands suggests the coexistence of different adsorbate states.

4. Conclusion

The adsorption of acetaldehyde, methyl acetate, ethyl acetate, and methyl trifluoroacetate on silica proceeds through the formation of hydrogen bonds that involve the donation of electron density from the lone-pair orbital in the carbonyl oxygen to the hydrogen atom(s) in surface hydroxyl groups. Interactions between the carbonyl and hydroxyl groups cause shifts to lower wavenumbers by 130–350 and 25–120 cm^{-1} of infrared bands associated with C=O and O–H stretching modes, respectively. These molecules primarily form two hydrogen bonds per adsorbate at high coverages. On the basis of microcalorimetric and thermal-desorption measurements, these hydrogen bonds have an average energy of 34 ± 4 kJ/mol in the cases of methyl and ethyl acetate adsorption, and a strength of 27 ± 4 kJ/mol per bond for acetaldehyde or methyl trifluoroacetate adsorption. Heats of ester adsorption as high as 96 kJ/mol are measured microcalorimetrically at surface coverages below 100 μmol/g, and these high heats are assigned, based on DFT calculations and spectroscopic studies, to the formation of three, and perhaps four, hydrogen bonds per adsorbate, thereby involving the alkoxy oxygen once the carbonyl oxygen is saturated. Heats of acetaldehyde adsorption on silica at low coverages are measured to be as high as 86 kJ/mol, and, in combination with spectroscopic measurements, these high heats are assigned to the oligomerization of acetaldehyde, which eventually yields crotonaldehyde via aldol-condensation reactions. The molecules studied desorb from silica at a maximum rate at temperatures from 325 to 400 K, and they can be removed completely by evacuation at 573 K.

Acknowledgements

The authors wish to acknowledge the financial support of the Office of Basic Energy Sciences of the Department of Energy and the National Center for Clean Industrial and Treatment Technologies, as well as GEM and AOF fellowships awarded to MANS. The authors want to thank W.S. Millman for providing the cell used in our spectroscopic studies.

References

[1] W. Hill, H. Miessner, G. Öhlmann, J. Chem. Soc., Faraday Trans. 1 85 (1989) 691.
[2] R. Pestman, R.M. Koster, J.A.Z. Pieterse, V. Ponec, J. Catal. 168 (1997) 255.
[3] J.I. Kroschwitz, M. Howe-Grant, Encyclopedia of Chemical Technology, Wiley, New York, 1991.
[4] A.T. Bell, L.E. Manzer, N.Y. Chen, V.W. Weekman, L.L. Hegedus, C.J. Pereira, Chem. Eng. Progress 91 (1995) 26.
[5] R.P. Young, N. Sheppard, Trans. Faraday Soc. 63 (1967) 2291.
[6] R.P. Young, N. Sheppard, J. Catal. 7 (1967) 223.
[7] W. Hertl, M.L. Hair, J. Phys. Chem. 72 (1968) 4676.
[8] R.P. Young, N. Sheppard, J. Catal. 20 (1971) 340.
[9] G. Busca, J. Lamotte, J.-C. Lavalley, V. Lorenzelli, J. Am. Chem. Soc. 109 (1987) 5197.
[10] P. Ugliengo, V.R. Saunders, E. Garrone, Chem. Phys. Lett. 169 (1990) 501.
[11] M. Allian, E. Borello, P. Ugliengo, G. Spanò, E. Garrone, Langmuir 11 (1995) 4811.
[12] P.A. Elkington, G. Curthoys, J. Phys. Chem. 72 (1968) 3475.
[13] S.N. Cross, C.H. Rochester, J. Chem. Soc., Faraday Trans. 1 75 (1979) 2865.
[14] R. Schifferli, J. Cortes, J. Chem. Soc., Faraday Trans. 1 77 (1981) 1845.
[15] R. Schifferli, J. Cortes, J. Colloid Interface Sci. 79 (1981) 589.
[16] K. Marshall, C.H. Rochester, Faraday Disc. Chem. Soc. 59 (1975) 1975.
[17] K. Marshall, C.H. Rochester, J. Chem. Soc., Faraday Trans. 1 71 (1975) 1754.
[18] R.P. Young, N. Sheppard, J. Catal. 20 (1971) 333.
[19] D.M. Griffiths, K. Marshall, C.H. Rochester, J. Chem. Soc., Faraday Trans. 1 70 (1974) 400.
[20] S.N.W. Cross, C.H. Rochester, J. Chem. Soc., Faraday Trans. 1 74 (1978) 2130.
[21] C.H. Rochester, D.-H. Trebilco, J. Chem. Soc., Faraday Trans. 1 75 (1979) 2211.
[22] N. Cardona-Martínez, J.A. Dumesic, J. Catal. 125 (1990) 427.
[23] N. Cardona-Martínez, J.A. Dumesic, Adv. Catal. 38 (1992) 149.
[24] A.D. Becke, J. Chem. Phys. 98 (1993) 5648.
[25] W.J. Hehre, L. Radom, P.V.R. Schleyer, Ab Initio Molecular Orbital Theory, Wiley, New York, 1986.
[26] W. Kohn, A.D. Becke, R.G. Parr, J. Phys. Chem. 100 (1996) 12974.
[27] T. Ziegler, Chem. Rev. 91 (1991) 651.
[28] M.J. Frisch, G.W. Trucks, H.B. Schlegel, P.M.W. Gill, B.G. Johnson, M.A. Robb, J.R. Cheeseman, T. Keith, G.A. Petersson, J.A. Montgomery, K. Raghavachari, M.A. Al-Laham, V.G. Zakrzewski, J.V. Ortiz, J.B. Foresman, J. Cioslowski, B.B. Stefanov, A. Nanayakkara, M. Challacombe, C.Y. Peng, P.Y. Ayala, W. Chen, M.W. Wong, J.L. Andres, E.S. Replogle, R. Gomperts, R.L. Martin, D.J. Fox, J.S. Binkley, D.J. Defrees, J. Baker, J.P. Stewart, M. Head-Gordon, C. Gonzalez, J.A. Pople, Gaussian 94 (Revision C.2), Gaussian, Pittsburgh, PA, 1995.
[29] C. Peng, P.Y. Ayala, H.B. Schlegel, M.J. Frisch, J. Comp. Chem. 17 (1996) 49.
[30] G.M. Zhidomirov, V.B. Kazansky, Adv. Catal. 34 (1986) 131.
[31] J. Sauer, Chem. Rev. 89 (1989) 199.
[32] J. Sauer, P. Ugliengo, E. Garrone, V.R. Saunders, Chem. Rev. 94 (1994) 2095.
[33] R.J. Cvetanovic, Y. Amenomiya, Adv. Catal. 17 (1967) 103.
[34] R.S. McDonald, J. Phys. Chem. 62 (1958) 1168.
[35] P. Hoffmann, E. Knözinger, Surf. Sci. 188 (1987) 181.
[36] B.C. Bunker, D.M. Haaland, K.J. Ward, T.A. Michalske, W.L. Smith, J.S. Binkley, C.F. Melius, C.A. Balfe, Surf. Sci. 210 (1989) 406.
[37] O. Sneh, S.M. George, J. Phys. Chem. 99 (1995) 4639.
[38] D.A. Sweigart, D.W. Turner, J. Am. Chem. Soc. 94 (1972) 5592.
[39] A.C. Legon, D.J. Millen, J. Chem. Rev. 86 (1986) 635.
[40] A.C. Legon, D.J. Millen, Acc. Chem. Res. 20 (1987) 39.
[41] J.B. Foresman, Æ. Frisch, Exploring Chemistry with Electronic Structure Methods, 2nd edn., Gaussian, Pittsburgh, PA, 1996.
[42] K.B. Wiberg, V. Walters, S.D. Colson, J. Phys. Chem. 88 (1984) 4723.
[43] B. Nikolova, J. Mol. Struct. 222 (1990) 337.
[44] W.O. George, T.E. Houston, W.C. Harris, Spectrochimica Acta A 30 (1974) 1035.
[45] T.-K. Ha, C. Pal, P.N. Ghosh, Spectrochimica Acta A 48 (1992) 1083.
[46] M.I. Redondo, M.V. García, M.A. Raso, W.A.P. Luck, J. Mol. Struct. 218 (1990) 213.
[47] G.A. Crowder, D. Jackson, Spectrochimica Acta A 27 (1971) 1873.
[48] G.A. Crowder, J. Fluorine Chem. 1 (1971) 219.
[49] G.I.L. Jones, T.D. Summers, N.L. Owen, J. Chem. Soc., Faraday Trans. 2 70 (1974) 100.
[50] I.N. Levine, Quantum Chemistry, 4th edn., Prentice-Hall, Englewood Cliffs, NJ, 1991.
[51] C.P. Sosa, J.E. Carpenter, J.J. Novoa, in: B.B. Laird, R.B. Ross, T. Ziegler (Eds.), Chemical Applications of Density-Functional Theory, Chap. 9, American Chemical Society, Washington, DC, 1996.